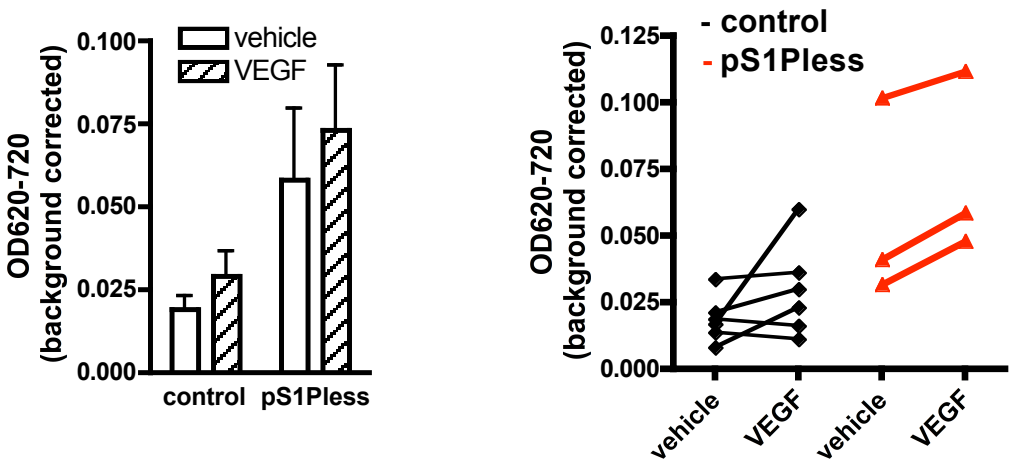

Supplementary Figure 1: Basal and VEGF-induced Evans blue leak in a Miles assay. Anesthetized mice were shaved free of back hair, injected i.v. with 100 µL filtered 1 % Evans blue/saline, and, 5 minutes later, injected intradermally with 100 ng of mouse $VEGF_{164}$ (R&D systems) in 50 µL Hanks/BSA at three sites evenly distributed along the right flank and Hanks/BSA control at three sites along the left flank. Thirty minutes later, mice were perfused with saline via the left ventricle to remove intravascular Evans blue. Pen-marked injection sites and control skin from untreated regions were excised with 8 mm skin biopsy punches and extracted in 0.5 mL of formamide at 55°C overnight. Evans blue content was determined as OD_{620}- OD_{720} of the formamide extract after correction for median OD of untreated skin from mice of the same genotype at both wavelengths. Left: mean +/- SEM. Right: Paired data, left flank to right flank for an individual mouse. Note increased Evans blue extravasation both at baseline and after VEGF in pS1Pless mice relative to controls.

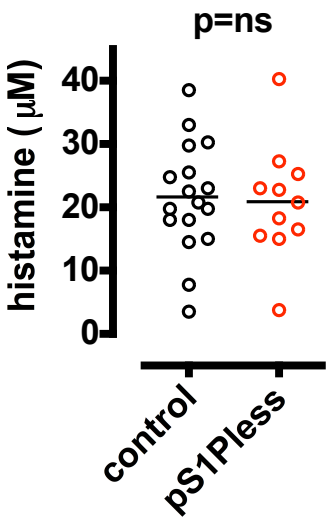

Supplementary Figure 2: Plasma S1P deficiency does not alter histamine levels during passive systemic anaphylaxis. Plasma histamine levels 90 seconds after DNP-albumin challenge in PSA model (see Methods) as determined by histamine ELISA (Immunotech, Marseille, France) performed according to the manufacturer's instructions. Plasma histamine levels were less than 0.3 μM in the absence of PSA challenge. p value was determined by student's t-test. Each point represents data for a separate mouse; horizontal bar denotes mean.

A complex role for sphingosine kinases in the regulation of mast cells and histamine secretion was recently described (Olivera A. et al, *Immunity* **26**,287-297 (2007). Olivera and colleagues reported decreased release of cytokines and granule constituents from fetal liver-derived mast cells from *Sphk2*$^{-/-}$ but not *Sphk1*$^{-/-}$ embryos, suggesting a positive role for Sphk2 in release of mast cell mediators. They also reported an ~30% decrease in plasma histamine levels after PSA in *Sphk1*$^{-/-}$ but not *Sphk2*$^{-/-}$ mice, as well as a strong correlation between plasma S1P and histamine levels after PSA. Plasma histamine and S1P levels were apparently determined after induction of anaphylaxis. Thus, it is possible that the strong correlation in plasma levels reflects, at least in part, secretion of both in response to anaphylactic mediators. While the ranges of histamine levels in the control and *Sphk1*$^{-/-}$ groups overlapped, median levels were ~30% different and this was statistically significant. The lack of an effect on histamine levels seen above in pS1Pless mice at plasma S1P levels significantly lower than those noted in the *Sphk1*$^{-/-}$ mice in the Olivera study suggest that plasma levels of S1P per se are probably not an important determinant of histamine release. Loss of S1P supplied by Sphk1 to other compartments or other consequences of loss of Sphk1 may explain the Olivera study's findings.

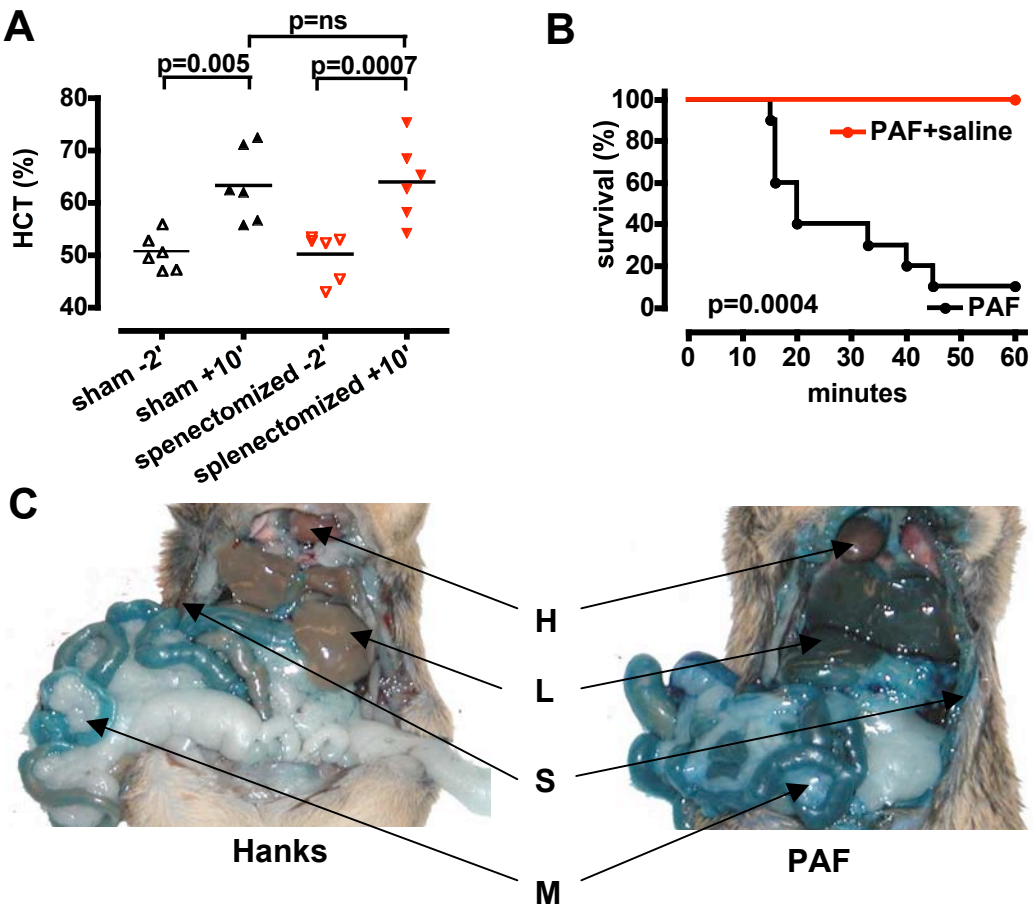

Supplementary Figure 3: Characterization of the PAF model. (**A**) Hematocrit (HCT) was measured before and 10 min after PAF (40 μg/kg PAF i.v.) in splenectomized or sham-operated mice. p values were determined by student's t-test (statistical comparisons as indicated), horizontal lines show mean values. Note that HCT increase was not altered by splenectomy, consistent with its being due to hemoconcentration rather than contraction of spleen and "autotransfusion". Each point represents data for a separate mouse; horizontal bar denotes mean. (**B**) Intravenous fluid resuscitation (0.5 ml saline at 7 minutes) of mice from lethal responses to 40 μg/kg PAF. p value determined by log rank test. (C) Evans blue leak in response to PAF challenge in wild-type mice. Evans blue/Saline (1 mg/ 100 μl) was administered i.v. with PAF (40 μg/kg) or vehicle control. Ten minutes later, intravascular Evans blue dye was removed by saline perfusion. H, heart; L, liver; S, skin; M, mesentery. Note increased Evans blue extravasation after PAF in multiple organs.

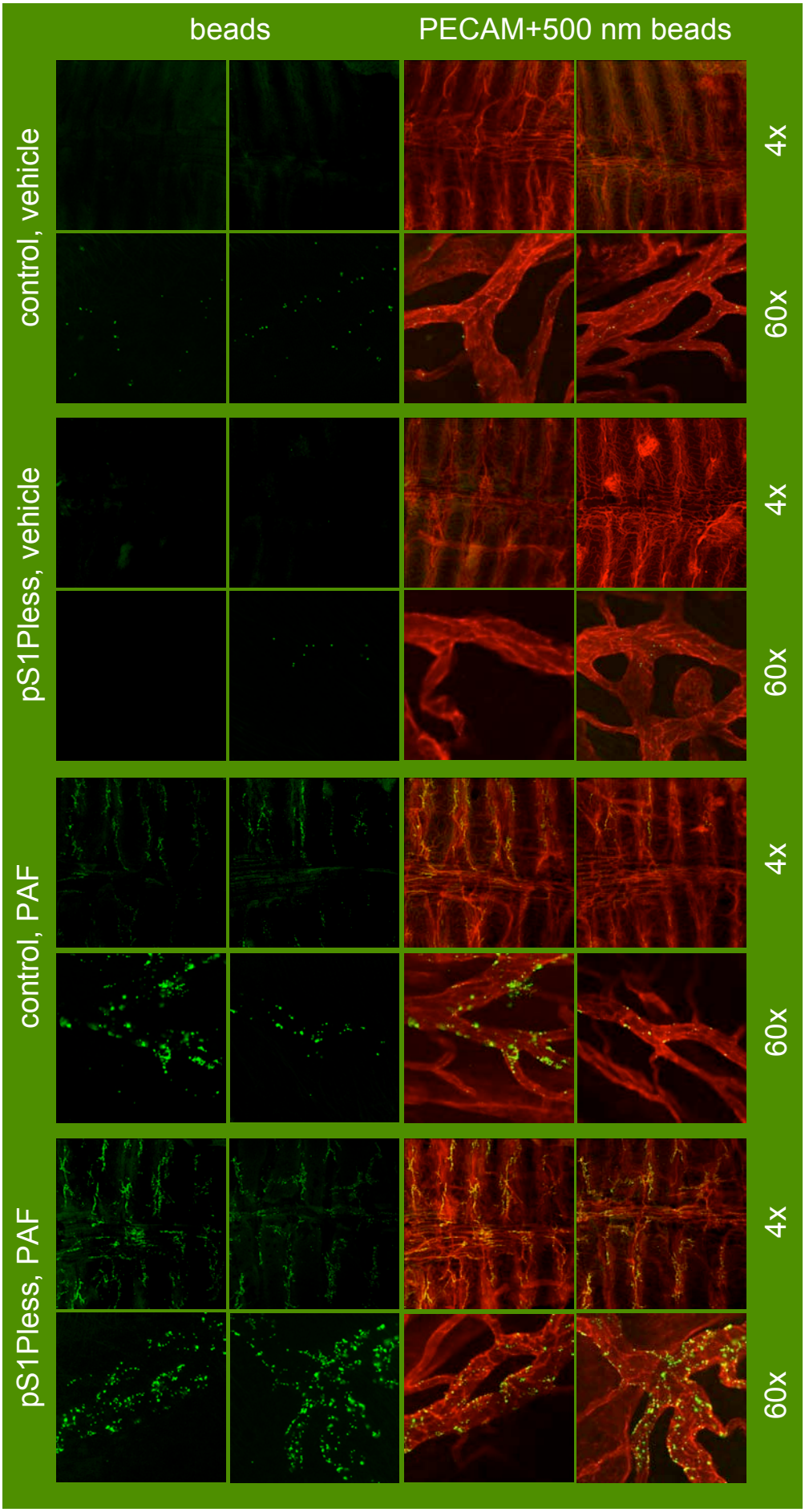

Supplementary Figure 4: pS1Pless mice exhibit increased extravasation of fluorescent microspheres via interendothelial gaps. Additional representative images to complement Figure 4 are shown. Control and pS1Pless mice were injected intravenously with 500 nm fluorescent microspheres together with PAF (20 μg/kg) or vehicle as indicated, then perfused 3 minutes later with saline then with fixative. Tracheae were removed, wholemount immunostained for the endothelial marker PECAM, opened, laid flat and imaged using confocal fluorescence microscopy. Minimal leak of microspheres was observed in vehicle-treated mice of either genotype (top four rows). Accumulation of microspheres was noted in venules in PAF-treated control mice but was less that that in PAF-treated pS1Pless mice; a rare large accumulation is shown (row 6 from top/column 3 from left). Venules with multiple and large accumulations were common in PAF-treated pS1Pless mice (bottom). Magnification refers to objective used.

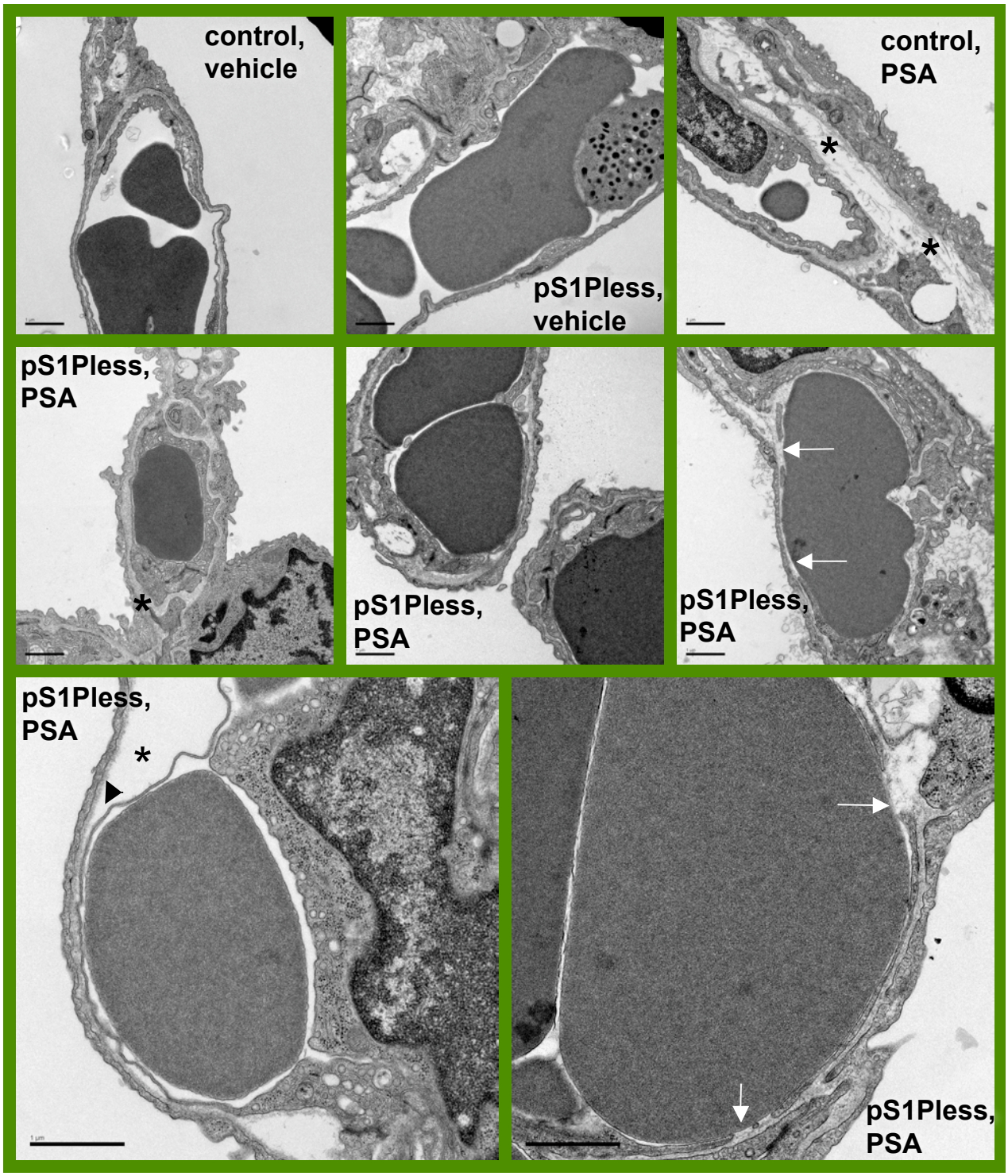

Supplementary Figure 5: Transmission electron microscopy (TEM) of lung. Mice were anesthetized 2 min after PSA induction. At 8 min, they were perfused with 0.1M sodium cacodylate buffer pH 7.4. At 18 min, they were perfused with 2% glutaraldehyde/1% PFA in cacodylate buffer (fix). At 33 min, trachea were instilled at 20 cm H2O with fix with the chest cavity intact. Heart and lung were collected en bloc and fixed at 4 ºC overnight, then processed for TEM by standard techniques. Alveolar capillaries showed apparent basement membrane edema (asterisk) in both control and pS1Pless mice. Apparent hemoconcentration and vasoconstriction (RBCs packed against endothelium) was more dramatic in pS1Pless mice, which also showed more common and prominent endothelial gaps (arrows) and endothelial thinning and detachment (arrowhead). Scale bars = 1 μm.

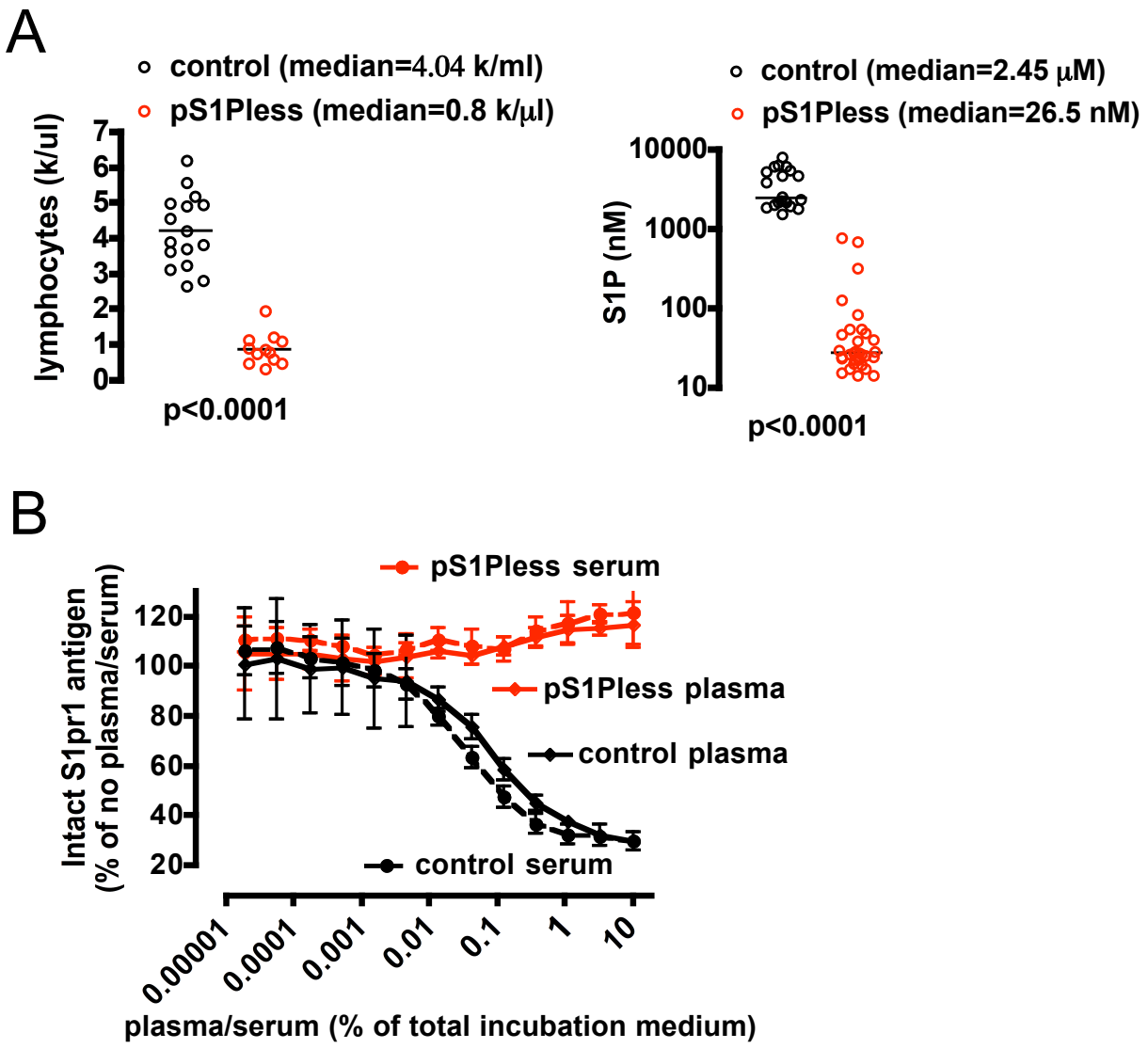

Supplementary Figure 6. (**A**) Peripheral lymphocyte counts and plasma S1P levels in control and pS1Pless mice. Lymphocyte counts were determined using a Hemavet (DREW Scientific). S1P levels were measured by mass spectrometry as described (15). Based on these data, lymphocyte counts and S1P levels were used as an index of efficient excision of the Sphk1 floxed allele after poly(I:C) induction of Mx1-Cre+:*Sphk1*fl/-:*Sphk2*$^{-/-}$ mice (pS1Pless mice). The occasional induced mouse with lymphocyte counts >2000/ul or plasma S1P levels above 200nM was excluded from study. Each point represents data for a separate mouse; horizontal bar denotes mean. (**B**) S1P levels were measured in serum, which contains platelet-released S1P, and platelet-poor plasma-derived serum ("plasma") from pS1Pless and control mice using downregulation of surface S1P1 from receptor-expressing WEHI cells as a bioassay. Results using this assay correlated well with mass spectrometry, but the bioassay was more sensitive (15). Note that control serum had approximately twice the level of S1P as control plasma, but no S1P activity was detected in either serum or plasma samples from pS1Pless mice. These results suggest that platelets do not contribute significant S1P to plasma in pS1Pless mice, presumably because platelets and other cells of hematopoietic origin do not make S1P in these mice. Mean & SD is shown, n=3.

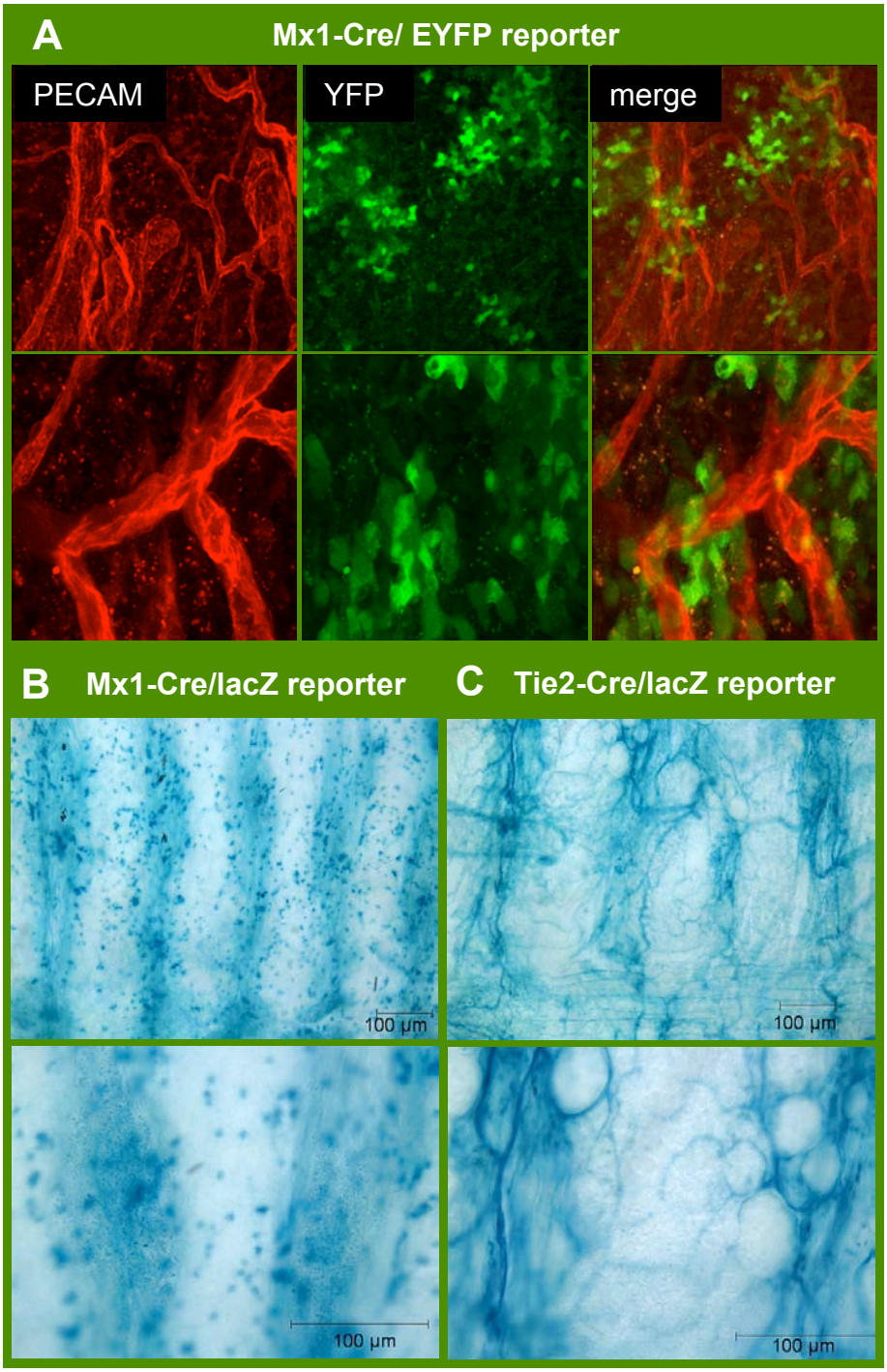

Supplementary Figure 7: Mx1-Cre does not cause efficient excision of reporter alleles in endothelial cells with the induction protocol used. Litters from Mx1-Cre transgenic mice crossed to either ROSA26 *Lox*-STOP-*Lox* EYFP or ROSA26 *Lox*-STOP-*Lox* β-galactosidase (lacZ) reporter mice were treated perinatally with poly (I:C). Trachea from Mx1-Cre+:ROSA26 *Lox*-STOP-*Lox* EYFP (**A**), Mx1-Cre+:ROSA26 *Lox*-STOP-*Lox* lacZ (**B**) and Tie2-Cre+:ROSA26 *Lox*-STOP-*Lox* lacZ (**C**) are shown. (**A**) Confocal fluorescence microscopy of trachea stained for PECAM, an endothelial marker (red), and EYFP (green). Green cells, probably hematopoietic in origin, did not co-localize with PECAM staining, arguing against endothelial excision. Higher magnification images are in lower panel. Similar results were obtained in (**B**) brightfield microscopy of trachea from poly (I:C)-induced Mx1-Cre+/lacZ reporter mice stained for lacZ activity (blue) and cleared in Benzyl Alcohol/Benzyl Benzoate. (**C**) positive control showing endothelial expression of Cre-excision reporter when Tie2-Cre was crossed to the reporter line used in (**B**). Lower panels show higher magnification.

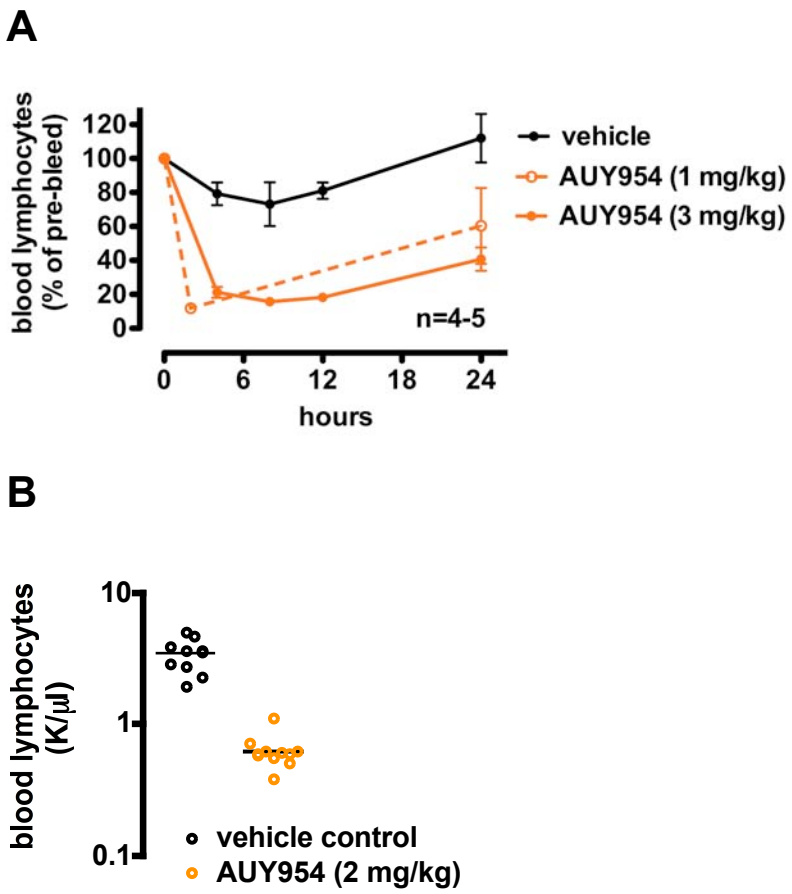

Supplementary Figure 8: Intravenous AUY954 rapidly induces reversible decreases in blood lymphocyte counts. (**A**) Time-course of peripheral lymphocyte counts after AUY954 i.v. injection. (**B**) Lymphocyte counts 5h after i.v. injection with 2mg/kg AUY95, the dose and approximate time used for the prolonged AUY954 exposure study in Fig. 5A-C. Note log scale. Each point represents data for a separate mouse; horizontal bar denotes mean.

GPCR	mRNA
S1pr1	100
Par1	98
S1pr3	17
S1pr2	14
Par2	6
Par4	3

Supplementary Table 1. Abundance of selected GPCR mRNAs in purified mouse endothelial cells relative to S1pr1. We quantitated mRNA levels for 353 of the 371 nonodorant GPCRs in mouse in endothelial cells purified from neonatal mouse skin using TaqMan RT-PCR. Par1 and S1pr1 were the most abundant GPCR mRNAs in these preparations, with levels only 8-fold below GAPDH. Other S1P receptors and PARs were also expressed above background but at lower levels. Data were normalized to ΔCt for S1pr1 (defined as 100%). The endothelial cell preparations used were of course a mixture of cells from different vessel types, and it is possible that relative expression levels differ by subpopulation.